Published in final edited form as:
Cancer Res. 2014 December 1; 74(23): 6968–6979. doi:10.1158/0008-5472.CAN-13-3369.

ATR inhibitors VE-821 and VX-970 sensitize cancer cells to topoisomerase I inhibitors by disabling DNA replication initiation and fork elongation responses

Rozenn Jossé[1], **Scott E. Martin**[2], **Rajarshi Guha**[2], **Pinar Ormanoglu**[2], **Thomas D. Pfister**[3], **Philip M. Reaper**[4], **Christopher S. Barnes**[4], **Julie Jones**[4], **Peter Charlton**[4], **John R. Pollard**[4], **Joel Morris**[5], **James H. Doroshow**[1,5], and **Yves Pommier**[1,*]

[1]Developmental Therapeutics Branch and Laboratory of Molecular Pharmacology, Center for Cancer Research, National Cancer Institute, NIH, Bethesda, MD

[2]Division of Pre-Clinical Innovation, National Center for Advancing Translational Sciences (NCATS), NIH, Rockville, MD

[3]Laboratory of Human Toxicology and Pharmacology, Applied/Developmental Research Directorate, Leidos Biomedical Research, Inc, National Laboratory for Cancer Research, Frederick, MD

[4]Vertex Pharmaceuticals (Europe) Ltd, Abingdon, Oxfordshire, UK

[5]Drug Synthesis and Chemistry Branch, Division of Cancer Treatment, Division of Cancer Treatment and Diagnosis (DTP-DCTD), NCI-NIH, Bethesda, MD

Abstract

Camptothecin and its derivatives, topotecan and irinotecan are specific topoisomerase I (Top1) inhibitors and potent anticancer drugs killing cancer cells by producing replication-associated DNA double-strand breaks, and the indenoisoquinoline LMP-400 (indotecan) is a novel Top1 inhibitor in clinical trial. To develop novel drug combinations, we conducted a synthetic lethal siRNA screen using a library that targets nearly 7,000 human genes. Depletion of ATR, the main transducer of replication stress came as a top candidate gene for camptothecin synthetic lethality. Validation studies using ATR siRNA and the ATR inhibitor VE-821, confirmed marked antiproliferative synergy with camptothecin, and even greater synergy with LMP-400. Single cell analyses and DNA fiber combing assays showed that VE-821 abrogates the S-phase replication elongation checkpoint and the replication origin-firing check point induced by camptothecin and LMP-400. As expected, the combination ofTop1 inhibitors with VE-821 inhibited the phosphorylation of ATR and Chk1; however, it strongly induced γH2AX. In cells treated with the combination, the γH2AX pattern changed overtime from the well-defined Top1-induced damage foci to an intense peripheral and diffuse nuclear staining, which could be used as response biomarker. Finally, the clinical derivative of VE-821, VX-970 enhanced the *in vivo* tumor response to irinotecan without additional toxicity. Akey implication of our work is the mechanistic

Corresponding author: Yves Pommier, Developmental Therapeutics Branch and Laboratory of Molecular Pharmacology, Center for Cancer Research, NCI, NIH, Bethesda, MD 20892. Tel.: 301-496-5944; pommier@nih.gov.

Conflict of interest statement: PMR, CB, JJ, PC and JRP are full time employees of Vertex Pharmaceuticals (Europe), Ltd.

rationale and proof-of-principle it provides to evaluate the combination of Top1 inhibitors with ATR inhibitors in clinical trials.

Keywords

DNA damage; replication; checkpoint; topotecan; irinotecan

Introduction

Topoisomerases are essential enzymes that catalyze the breaking and rejoining of the phosphodiester backbone to allow the unwinding and disentanglement of DNA during replication and transcription. Among them, Top1 produces transient single-stranded DNA breaks as catalytic intermediates that are referred to as Top1 cleavage complexes (Top1cc) (1). Anticancer Top1 inhibitors act by slowing down the reversal of Top1cc and the religation of DNA (2–4). Persistence of Top1cc leads to collisions with replication forks and transcription complexes, converting them into irreversible Top1 covalent complexes and DNA double-strand breaks, which, if not repaired are lethal. The anticancer activity of Top1 inhibitors is primarily related to replication damage by replication “run-off” and replication-mediated DNA double-strand breaks (3,5,6).

Camptothecin (CPT) and its derivatives are highly selective inhibitors of Top1, and the water-soluble derivatives, topotecan and irinotecan are effective anti-cancer drugs against a wide range of tumors. However, they are limited by their chemical instability, ABCG2- and MDR1-mediated efflux, the rapid reversibility of the Top1cc, and dose-limiting bone marrow and gastro-intestinal toxicity (3,5). To overcome these limitations, we have developed a novel class of Top1 inhibitors, the indenoisoquinolines (2), which are chemically stable, not substrates for the drug efflux membrane pumps, and produce persistent Top 1cc (7). LMP-400 (Indotecan, NSC-724998) is one of two indenoisoquinolines currently in phase I clinical trial.

The broad use of camptothecins and the potential of LMP-400 as a clinical agent raise the prospect of rationale drug combinations. To address this goal, we conducted abroad ranges iRNA-based screening to reveal targets that, when silenced, improve the efficacy of Top1 inhibitors. Using CPT and an apoptosis-targeted siRNA library, we recently demonstrated the feasibility of the approach and identified the kinase TAK1 (MAP3K7), which is involved in cancer cell growth and in the NFkB, p38, JNK pathways, as a novel synthetic lethal pathway for Top1-mediated DNA damage (8). In the present study, we extended this approach to more than 7,000 human genes with 4 independent siRNAs per gene, and identified siRNAs that were synthetically lethal withTop1 poisoning, prioritizing genes that can be validated with drugs in preclinical development. We focused on ATR (ataxia telangiectasia and Rad3-related protein kinase), a major signal transducer of the replication stress-induced DNA damage response (DDR), which functions in parallel with ATM (ataxia telangiectasia mutated), a major transducer of the DNA double-strand break responses (9–12).

ATR is activated in response to replication stress (single-stranded DNA associated with replication complexes and stalled replication forks) induced by UV, hydroxyurea or chemotherapeutic drugs such as camptothecins. In turn, ATR activates the cell cycle kinase Chk1 by phosphorylation (at serine 345), leading to a suppression of origin firing and DNA elongation, and cell cycle arrest in S/G, which promote repair and prevent premature mitosis, thereby maintaining genomic stability (9,10).

Potent and selective ATR inhibitors are in clinical development (13–17) with the rationale to target cancer cells under replication stress resulting from oncogene addiction (14,18,19) or chemotherapeutic replication inhibitors such as Top1 inhibitors or gemcitabine (20–22). In the present study, we explore the molecular and preclinical rationale for combining Top1 inhibitor with ATR inhibitors.

Materials and methods

Cell lines, chemicals, and drugs

HT29 and COLO 205 colon and MDA-MD-231 breast carcinoma cells were grown in RPMI medium with 10% fetal bovine serum (FBS; Gibco-BRL) at 37°C in 5% CO2. HT29 and MDA-MB-231 cells, CPT, LMP-400 and VE-821 were obtained from the Developmental Therapeutics Program (DCTD, NCI) where cells were authenticated by short tandem repeat DNA finger printing. COLO 205 colorectal adenocarcinoma cells were purchased from the American Type Culture Collection (ATCC). HCT116 wild-type and p53 knockout cells were given by Bert Vogelstein (Johns Hopkins University). All the cell lines were confirmed with the absence of Mycoplasma contamination (MycoAlert; Lonza). VX-970 (VE-822) was produced by Vertex Pharmaceuticals.

siRNA screening

For transfections, 20 μL of serum free media containing Lipofectamine RNAiMax (0.05 μL) was added to wells of 384 well plates (Corning 3570) containing siRNA (0.8 pmol) Lipid and siRNA were allowed to complex for 45 min at ambient temperature before addition of 600 MDA-MB-231 cells to yield final transfection mixtures containing 20 nM siRNA in RPMI, 10% FBS. CPT (20 nM, ~EC_{30}) or vehicle (0.1% DMSO) was added to the entire plate 48 h post-transfection and viability (CellTiter Glo, Promega) was assayed 72 h later on a PerkinElmer Envision 2104 Multilabel Reader.

The druggable genome screening was conducted using the Qiagen human druggable genome library version 4.1, which targets nearly 7,000 human genes with ~4 siRNAs per gene. Each siRNA is arrayed in an individual well. Qiagen's All Stars Negative control and Qiagen's All Stars Cell Death control were incorporated on all screening plates for normalization and as positive transfection control, respectively. Plates were rejected and rescreened if they exhibited an assay z′-factor of less than 0.4 or other apparent defects. Follow-up dose response tests were carried under analogous assay conditions.

To select candidate genes modulating CPT activity, the log2 ratio of vehicle-treated cell viability (% siNeg) to CPT-treated cell viability (% siNeg) was calculated for each siRNA. Redundant siRNA Analysis (RSA) (23) was performed on the ratios to rank gene candidates

in terms of their ability to sensitize MDA-MB-231 to CPT. RSA rankings can be found in Supplemental Table S1. All screen data have been deposited on PubChem (AID 743121).

Ingenuity Pathway and STRING (24) analyses were performed to identify enriched pathways and protein-protein interactions among these 42 candidates. For IPA, a core analysis was performed using only direct relationships and used the ~7,000 genes represented in the screen as background. For STRING, relationships were mined using only experiment and database determined relationships of at least “medium confidence”.

Cytotoxicity

Cells were seeded in 96-well plates 24 h before drug addition. After a 72 h treatment, cell survival was determined using the ATPlite® 1 step kit (PerkinElmer Life Sciences). Luminescence was measured by an Envision 2104 Multilabel Reader. Synergism was assessed using the CompuSyn Software.

Analyses of EdU incorporation, cell cycle and apoptosis

HT29 cells were incubated with 50μM 5-ethynyl-2′-deoxyuridine (EdU) for 30 min before adding Top1 inhibitors for 1h. Cells were harvested 18 hour-post Top1 inhibitors. EdU was detected by flow cytometry (Click-iT EdU Alexa Fluor 647 Flow Cytometry Assay; Invitrogen), and DNA using propidium iodide (PI). Apoptotic cells were detected 48 hour-post Top1 inhibitors using Annexin V/PI co-staining (FITC Annexin V Apoptosis kit, BD Biosciences). Samples were analyzed on a FACS can flow cytometer (Becton Dickinson).

Immunofluorescence microscopy staining of replication foci using CldU and IdU

HT29 cells were grown in four-well chamber slides (Nalge-Nunc) and labeled with 100 μM chlorodeoxyuridine (CldU) or iododeoxyuridine (IdU) for 45 min. Slides were prepared (6) and images visualized with a Zeiss LSM 780 confocal microscope.

DNA fiber assays

Molecular combing was performed as described (6). Briefly, at the end of the CldU pulse, trypsinized cells were embedded in low-melting agarose. After digestion with β-agarase (New England Biolabs), DNA was combed on silanized surfaces (Microsurfaces, Inc.) and replicons were detected with anti-IdU and anti-CldU antibodies. Images were captured with the software Attovision using the epifluorescence microscope Pathway (Becton Dickinson). Signals were measured using ImageJ (open source from National Cancer Institute, NIH) with custom-made modifications.

Immunoblotting

Total cell lysates were electrophoresed on 4–20% Tris-glycine or 3–8% Tris-acetate polyacrylamide gels, and transferred onto nitrocellulose membranes. Antibodies against GAPDH, ATR and pS345-Chk1 were obtained from Cell Signaling Technologies, γH2AX and pT68-Chk2 from Abcam and Top1 from BD Biosciences. Antibody against pT1989-ATR was generated by the Pharmacodynamics Assay Development and Implementation Section (PADIS) of the Laboratory of Human Toxicology and Pharmacology at the National

Laboratory for Cancer Research (Frederick, MD). After incubation with secondary antibody, signals were detected by enhanced chemiluminescence (Pierce).

IdU and γH2AX staining

After incubation with 100 μM IdU for 75 min with or without drugs for 1 h, HT29 cells were fixed at different time intervals with 4% paraformaldehyde for 10 min. Slides were prepared (6) and images visualized by Zeiss LSM 780 confocal microscope.

Xenografts

MF1 athymic, nude mice were treated in accordance with the Animal (Scientific Procedures) Act and the UKCCCR Guidelines for the Welfare of Animals in Experimental Neoplasia. Mice weighing 20–30 g (Harlan UK Ltd Lough borough, UK) were inoculated subcutaneously with 1×10^7 COLO205 cells in 100μl of a serum-free media and matrigel mixture (1:1). When the tumors reached about 250 mm^3 the mice were randomized in groups of 8 animals. VX-970 (VE-822, 60 mg/kg in a solution in 10% VitE TPGS) was administered by oral gavage on days 0, 1 and 2 of each 4-day cycle. Irinotecan (20 mg/kg or 40 mg/kg in PBS) was administered by intraperitoneal bolus injection on day 0 of each 4-day cycle. The control group was treated with vehicle (10% VitE TPGS in water) on days 0, 1 and 2 of each 4-day cycle. A total of 4 treatment cycles were given. Tumors were measured twice a week by caliper and volumes calculated using the formula (length × width2)/2. Body weight was assessed twice a week.

Results

RNAi screening identifies ATR as a top synthetic lethal gene for Top1 inhibitors

To determine pathways and associated drug-targets to improve the use of Top1 inhibitors, we conducted a druggable genome screen targeting nearly 7,000 human genes in MDA-MB-231 cells (8). To select candidate genes that modulate CPT activity, the $\log_2$ ratio of vehicle-treated to CPT-treated cell viability was calculated for each siRNA and Redundant siRNA Analysis (RSA) (23) was used to rank gene candidates for their ability to sensitize to CPT. RSA identified 42 candidates with $p \leq 0.001$ (Supplemental Table S1). Ingenuity Pathway Analysis (IPA) on these top candidates revealed an expected enrichment in canonical cell cycle and DNA repair related pathways (Supplemental Table S2), and both IPA and STRING (24) identified enrichments for known protein-protein interactions (Fig. 1A and Supplemental Fig. S1). Evasion of apoptosis represents one of the fundamental hallmarks of cancer and can be driven by upregulation of pro-survival factors. Accordingly, we found that several anti-apoptotic factors ranked high in the screen. They included BCL2L1 (BCLXL) and the complex comprising MAP3K7 (TAK1), MAP3K7IP2 (TAB2) and TRAF6, which is consistent with our prior screen (8). These results indicated that the screen identified relevant genes.

To further investigate top candidate genes, the effects of siRNAs were examined with CPT concentration-responses. Follow-up was performed in two rounds. The first involved testing many of the same sequences from the primary screen, plus additional siRNAs from the same vendor (Qiagen). In all, at least four sequences were tested for 79 of 133 genes scoring p <

0.005 by RSA (Supplemental Table S3). In the second round, three additional siRNAs were obtained from a different vendor (Ambion) for 47 of the candidate genes to further distinguish the most robust hits and reduce the likelihood of false positives from off-target effects. Figure 1B lists those with more than half of ≥ 7 siRNAs yielding > 4-fold sensitization. The corresponding curves can be found in Supplementary Figure S2. ATR was among the most potent and robust targets, and additional testing showed that depletion of ATR similarly affected LMP-400 (Fig. 1C). Because of the ongoing development of clinical ATR and Top1 inhibitors, and our interest in Top1-mediated DNA replication damage and S-phase checkpoint regulation (6,25,26), the remaining part of our study focuses on the combination of ATR inhibitors with CPT and LMP-400.

VE-821 potentiates the cytotoxicity of both camptothecin and LMP-400

VE-821 was chosen for our molecular analyses because of its well-documented effects on ATR (13,15,21). Cells were exposed to CPT or LMP-400 for 1 hbecauseTop1 inhibitors are usually administered as short-time infusions. Yet, they produce extended cell cycle arrest and checkpoint responses (6,26,27). VE-821 treatments were started together with the Top1 inhibitors but continued after Top1 inhibitor removal to maximize the impact of check point inhibition (6,25). Three colon carcinoma cell lines were examined in addition to the MDA-231 breast cancer cells: HT29 and a pair of isogenic HCT116 cells wild-type and p53 knockout to study the contribution of p53 to the potentiation of drug lethality.

VE-821 alone had minimal effect on cell viability up to 10 μM (Fig 2). Consistent with the results obtained in cells depleted for ATR by RNAi (see Fig. 1C), VE-821 sensitized MDA-MB-231 cells to both CPT and LMP-400 (Fig. 2A, upper and lower panels). The impact of the combination was stronger in HT29 (Fig. 2B) and in TP53-deficient HCT116 cells (Fig. 2D) than in MDA-MB-231 and HCT116 cells (Figs. 2C). It was also more pronounced for LMP-400 than CPT. Synergy was evaluated (28) using the CompuSyn software at the non-cytotoxic concentration of 1 μM VE-821. The results are illustrated with CI (combination index) values below 1, as observed in all cell lines for both CPT and LMP-400 except for the TP53-proficient HCT116 cells (Fig. 2E). Because HT-29 cells were used in our previous cell cycle checkpoint studies (6,25–27), we performed the following molecular analyses in HT29 cells using 1 μM concentration for both the Top1 and ATR inhibitors.

VE-821 abrogates the intra S-phase checkpoint induced by CPT and LMP-400, and induces apoptosis

Top1 inhibitors alone produced a marked delay in S phase progression (6,7,26):18 h-post treatment with CPT and LMP-400, cells accumulated in late and mid S-phase, respectively (Fig. 3B, left panels). VE-821 abrogated this S-phase delay, enabling cells to move through the G2/M checkpoint after CPT while accumulating in G2/M after LMP-400 (Fig. 3B, right panels). The more pronounced cell cycle effect of LMP-400 is consistent with its more potent and persistent Top1 inhibition and greater cytotoxicity (see Fig. 2) (7).

To further examine the effects of VE-821 on cell cycle progression, and because Top1 inhibitors selectively target replicating cells, we followed the cells that were in S-phase during the Top1 inhibitor treatments using EdU pulse-labeling (6) (Fig. 3A). FACS profiles

of EdU incorporation versus DNA content revealed the progression of control cells and VE-821-treated cells through the cell cycle, indicating their normal progression through G2/M toward the next S phase (Fig. 3C, upper panels). As expected, CPT and LMP-400 produced a marked delay in S-phase progression with cells blocked in G2 without advancing to the next cell cycle (Fig. 3C, left panels). The non-EdU labeled cells (i.e. those that were not in S-phase at the time of Top1 inhibitor treatment) progressed also very slowly with more cells in G2 after CPT treatment than in the control cells. In the case of LMP-400, most of the non-EdU-labeled cells were in G2, and only few in G1, indicating that only few cells were able to initiate a new cell cycle. VE-821 allowed cell cycle progression of the cells that had been targeted in S-phase by the Top1 inhibitors (Fig. 3C, right panels); the cells were more broadly distributed throughout the cell cycle, with a fraction of labeled cells having progressed through G2/M and being in S-phase of the next cell cycle. Together, these experiments demonstrate that VE-821 efficiently abrogates the intra-S phase and G2 checkpoints induced by CPT- and LMP-400.

Induction of apoptosis using Annexin V/PI co-staining was also monitor (Fig. 3D). Consistent with the survival experiments (Fig. 2), the combination VE-821 plus Top1 inhibitors increased the fraction of early apoptotic cells (Annexin V positive/PI negative; from 4.5% to 26% for CPT and 16.6% to 28.7% in the case of LMP-400).

Uninhibited DNA synthesis in preexisting replication foci and in new replication foci in cells treated with Top1 inhibitors and VE-821

CPT activates theChk1-dependent intra-S-phase checkpoint that inhibits the firing of late replication origins (6). To examine origin firing, we analyzed DNA replication foci by sequential pulse-labeling with CldU and IdU (Fig. 4A).

Figures 4B and 4E show representative images for untreated and VE-821-treated cells, respectively. After 8 h (the time interval between the two pulses), new replication foci formed while those that were active 8 h earlier did not in corporate IdU any longer. As a result, the green (CldU) and red (IdU) foci generally do not colocalize, demonstrating cell cycle progression through S phase.

In the absence of VE-821, CPT-and LMP-400-treated cells (Fig. 4C and D) showed a pronounced attenuation of IdU foci, demonstrating S-phase checkpoint with inactivation of late replication origins (6). By contrast, in the presence of VE-821, IdU foci were restored in spite of CPT or LMP-400 (Fig. 4F and 4G). Most CldU and IdU foci remained distinct, indicating initiation of new origins. Yet, in some cells, some CldU foci colocalized with IdU foci suggesting persistence of replication foci beyond 8 h. These results demonstrate that VE-821 blocks origin firing inhibition in cells treated with Top1 inhibitors.

VE-821 rapidly inhibits the DNA elongation check point induced by Top1 inhibitors

Together with inhibition of replication origin firing, CPT produces a rapid fork elongation response (6). To elucidate the effect of Top1 inhibitors and VE-821 on checkpoint control of replication fork progression, DNA fibers were analyzed to visualize single replicons (6,29). Cells were sequentially pulse-labeled with IdU and CldU. Top1 inhibitors were added during the CldU pulse, while VE-821 was present during both pulses (Fig. 5A).

Representative DNA replication forks are shown in Figure 5B. Newly synthesized DNA fibers emanating from replication origins fired before the IdU pulses were labeled in green. Contiguous with green tracts, red tracts correspond to DNA synthetized during the CldU pulse as replication continued.

In cells exposed to CPT or LMP-400 without VE-821, DNA synthesis during the CldU pulse was inhibited, resulting in short red tracks (Fig. 5B, left) (6,25). By contrast, in cells exposed to VE-821 DNA synthesis persisted during the second pulse (Fig. 5B, right). To quantify the impact of the combinations of CPT or LMP-400 with VE-821 on DNA replication fork progression, we analyzed the ratio of CldU to IdU pulses (Fig. 5C). In untreated cells or in cells exposed to VE-821 alone, the ratios were closed to 1 (1.17 and 1.07, respectively), indicating that replication fork velocity was comparable during each pulse. CPT and LMP reduced the CldU: IdU ratio to 0.52 and 0.34, respectively. This replication forks low down was abrogated by VE-821, as the ratio CldU: IdU shifted back to 0.98 and 1.02 for the combinations of VE-821 with CPT or LMP-400 respectively. These results demonstrate that VE-821 abrogates the DNA elongation checkpoint.

DDR molecular biomarkers induced by VE-281

Because VE-281 directly targets ATR (13,15) upstream from Chk1, we determined auto-phosphorylation of ATR on threonine 1989, a DNA damage activation site (30,31), and Chk1 phosphorylation on serine 345, which is mediated by ATR. We also determined histone H2AX phosphorylation on serine 139 (γH2AX), a validated pharmacodynamic biomarker for DNA damage and apoptosis (32–34).

CPT and LMP-400 quickly induced the rapid phosphorylation of Chk1, Chk2 and H2AX, while phosphorylation of ATR was delayed and best detectable after drug removal. Chk1 and ATR remained phosphorylated for 18 h after drug removal, consistent with the persistent checkpoint activation for hours after Top1 inhibitor removal (6,27). VE-821 inhibited the phosphorylation of both ATR and Chk1 without reducing Chk2 phosphorylation, confirming the specificity of VE-821 for ATR. Notably, VE-821 strongly induced γH2AX over time (Figs. 6B and 6C). LMP-400 showed more pronounced effects than CPT, consistent with the enhanced Top1 inhibitory potency of LMP-400 (7) (see also Figs. 1 and 2).

VE-821 markedly enhances γH2AX

Next we focused on γH2AX using single cell analyses (6) to determine the relationship between the γH2AX and DNA replication foci (labeled by short IdU pulses), and the possible induction of γH2AX pan-staining, as a hallmark of ATR-dependent replication stress (14,18) and apoptosis (34).

Consistent with previous results (6,7), in the absence of VE-821, CPT- and LMP-400-induced γH2AX foci mostly colocalized with DNA replication foci (Fig. 6D left panels second row and 5th row and Fig. 6E, right panels, top row). At the one-hour treatment time, VE-821 had no significant impact on CPT- or LMP-400-induced γH2AX foci intensity and distribution (Fig. 6D–E).

Next we examined the γH2AX response at later times in the presence and absence of VE-821. Consistent with the Western blotting results (Fig. 6B–C), in the absence of VE-821, CPT-induced γH2AX foci decreased over time while LMP-400-induced γH2AX foci were more persistent. Notably, in the presence of VE-821, the γH2AX pattern changed. Instead of well-defined foci, γH2AX staining became diffuse and appeared like a ring. This "γH2AX ring" increased over time (Fig. 6D, right panels). Figure 6E shows detailed images of a typical cell following LMP-400+VE-821 cotreatment, demonstrating that γH2AX accumulates at the periphery of enlarged nuclei without localization with the replication foci. Similar results were obtained with CPT, although with a lesser intensity. Together, these results demonstrate that ATR inhibition by VE-821 produces intense γH2AX pan staining.

In vivo potentiation of irinotecan by VX-970

To assess the effect of ATR inhibition on tumor responses to Top1 inhibitors, we used VX-970 (VE-822), which is a close analog of VE-821 with improved potency and absorption, distribution, metabolism and excretion (ADME) properties that make it usable *in vivo* as an ATR inhibitor (16,22). First we assessed the combined effect of VX-970 and the active metabolite of irinotecan, 7-ethyl-10-hydroxycamptothecin (SN-38) *in vitro* on COLO205 colorectal cancer cell viability. Strong synergy was observed between the two agents at concentrations of VX-970 as low as 80 nM; VX-970 decreased the half-maximal inhibitory concentration (IC50) of SN38 by ≥ 8-fold (Supplemental Fig. S3).

Next we tested the combination in mice bearing subcutaneous COLO205 tumors. Mice were treated with either irinotecan (dosed IP on day 0 of a 4 day cycle), VX-970 (dosed by oral gavage on days 0, 1 and 2 of each 4 day cycle) or the combination of the two together. After short periods of tumor growth, treatment with 20 mg/kg irinotecan led to 88% tumor growth inhibition and at the maximum tolerated dose of 40 mg/kg, complete tumor growth inhibition was observed (compared with starting tumor volumes, Fig. 7A, C). Although VX-970 had no impact on tumor growth when dosed as a single agent at 60 mg/kg, it was highly effective when dosed in combination with 20 mg/kg irinotecan, where substantial tumor regression was observed (29% at day 15 and 55% at the nadir on day 21). Notably, the anti-tumor activity for the combination was greater than that observed with irinotecan alone when dosed at its maximum tolerated growth (MTD). The combination was well tolerated with no increased body weight loss when compared with single agent irinotecan treatment (Fig. 7B).

Discussion

Although camptothecins are therapeutically effective, they are not curative as single agents and novel combinations are needed to improve their efficacy. In this study, we used siRNA screening to identify combinations of drug-targeted proteins and pathways. We identified significant candidate genes involved in apoptosis. BCL2L1, an anti-apoptotic member of the Bcl2 family, also known as BCLXL, whose expression is increased in various cancers (35,36) and which inhibits pro-apoptotic factors such as BAX and BAK (36), scored as a top sensitizer. Small molecule inhibitors of BCL2/BCL-XL such as Obatoclax or ABT-737 have

been used in monotherapy or in combination with various agents notably Top inhibitors (37,38). Depletion of TRAF6, MAP3K7 and MAP3K7IP2, three genes involved in NFkB activation and in a kinase complex comprising TAK1 (MAP3K7), TAB1, TAB2 (MAP3K7IP2) and TRAF6 (39), also sensitized to CPT. We also found RNF31 (HOIP), which activates the NFkB pathway through the polyubiquitylation of NEMO in the canonical IKK complex (40). These results are consistent with a previous screen (8).

The DNA damage sensing kinase, ATR, which was also among the top candidates, was chosen for further analyses as ATR inhibitors are entering clinical trials. After recognition of stalled replication forks, ATR regulates the intra S-phase checkpoint by stabilizing replication forks, regulating cell cycle and DNA damage repair (9,10). siRNA of three ATR targets: Chk1, BRCA1 and UPF1 (41) also scored as top candidates, as did the PPP2R1A subunit of the protein phosphatase PP2A, which is involved in the regulation of the cell cycle checkpoints (42).

As the primary cytotoxic mechanism of Top1 inhibitors in dividing cells is by generation of replication-fork collisions that convert Top1cc into irreversible DNA lesions (5), ATR and its downstream target, Chk1 are crucial factors for the DNA damage response to Top1 inhibitors (5,6,25). Accordingly, inhibition of ATR by siRNA or VE-821 and its clinical derivative VX-970, sensitized tumor cells to Top1 inhibitors. Loss of p53 influenced cell sensitivity to the combination of ATR and Top1 inhibitors as demonstrated in an isogenic system (14–16,43). However, cellular sensitivity did not strongly correlate with *TP53* mutational status in heterogeneous cell panels (16). Our results are in agreement with recent reports describing the sensitization of cancer cells to combinations of VE-821 with multiple agents including CPT, topotecan, etoposide, gemcitabine, cisplatin and ionizing radiation (15,20,21). Moreover similarly to the disruption of Chk1 by UCN-01, CHIR-24, and AZD7762 (6,25,26,44,45), disruption of ATR by VE-821 abrogated the cell cycle arrest induced by CPT and LMP-400. The addition of VE-821 forced progression through S-phase and G2/M for a proportion of the cells exposed to CPT, whereas the LMP-400-treated cells progressed through S-phase but were still not able to efficiently complete mitosis.

Single cell analyses of DNA replication foci using CldU: IdU sequential pulses revealed that the combination of VE-821 with Top1 inhibitors induced unscheduled DNA synthesis and allowed late-replicating chromosomal domains to initiate replication. Because each replication focus in immunohistochemistry experiments contains multiple origins, we utilized molecular combing (DNA fiber assays) to visualize single replicons (6,29) and measure the impact of ATR on the elongation of damaged replicons. We previously demonstrated that CPT and LMP-400 inhibit DNA elongation (6,25) but here, using comparable conditions, we show that LMP-400 is a more potent inhibitor of DNA elongation than CPT. Yet, VE-821 acted very rapidly to inhibit this checkpoint response elicited by CPT or LMP-400.

DNA double-strand breaks induced by Top1 inhibitors are mediated both by replication or transcription collisions (5,46). A recent study describing a method to quantify the spatial distance between γH2AX foci and replication factories using confocal microscopy, estimated a close relationship between γH2AX foci and replication factories (47). γH2AX

foci induced by LMP-400 were more persistent than those induced by CPT, which is consistent with the chemical stability and persistence of LMP-400-induced Top1cc after drug removal (7). As shown by immunoblotting, inhibition of ATR by VE-821 led to an accumulation of γH2AX induced by Top1 inhibitors while VE-821 by itself did not induce γH2AX. Previous reports (15,20,21,48) are in agreement with our findings showing phosphorylation of H2AX on Ser139 (γH2AX) by ATM and/or DNA-PK after stalled replication, especially in the absence of ATR (14,49). Furthermore, VE-821 has been shown to inhibit homologous recombination repair, as evidenced by a decrease in RAD51 foci (21).

A notable finding of the present study is the induction of intense"γH2AX rings" in cells cotreated with Top1 inhibitors and VE-821, starting a few hours post-Top1 inhibitors and followed by a pan staining that persisted until the formation of apoptotic bodies. Yet, this diffuse staining starting at the nuclear periphery is not initially associated with classical apoptotic markers. Rather, it may be related to the diffuse nuclear γH2AX staining induced by ATR inhibition, which was used as an endpoint in a high-throughput cell-based screen to identify ATR inhibitors (14). From a pharmacodynamic perspective, the intense γH2AX diffuse nuclear staining might be useful to evaluate combination therapy with Top1 and ATR inhibitors, and could be tested as a response biomarker in tumor samples, circulating tumor cells and surrogate tissues, such as plucked hairs (50). Based on our study, additional pharmacodynamic biomarkers for ATR inhibitors could be inhibition of Chk1 phosphorylation on Ser345 (21,48) and inhibition of ATR auto phosphorylation on threonine 1989.

Beyond its molecular and mechanistic insights, our study provides the proof of concept that ATR inhibitors are worthy of consideration for clinical trials in combination with Top1 inhibitors. Indeed, the clinical derivative of VE-821, VX-970 (16), showed remarkable synergism in combination with irinotecan, a widely used Top1 inhibitor. Further studies are warranted to examine VX-970 and other ATR inhibitors in combination with irinotecan, topotecan or the non-camptothecin indenoisoquinolines, such as LMP-400 and LMP-776 (2).

Supplementary Material

Refer to Web version on PubMed Central for supplementary material.

Acknowledgments

Our studies were supported by the NCI Intramural Program, Center for Cancer Research (Z01-BC006161 and Z01-BC006150), by the Federal funds from the National Cancer Institute, NIH under Contract No. HHSN261200800001E, and in part by the American Recovery and Reinvestment Act funds.

References

1. Pommier Y, Leo E, Zhang H, Marchand C. DNA topoisomerases and their poisoning by anticancer and antibacterial drugs. Chem Biol. 2010; 17(5):421–33. [PubMed: 20534341]
2. Pommier Y, Cushman M. The indenoisoquinoline noncamptothecin topoisomerase I inhibitors: update and perspectives. Mol Cancer Ther. 2009; 8(5):1008–14. [PubMed: 19383846]
3. Pommier Y. Drugging topoisomerases: lessons and challenges. ACS chemical biology. 2013; 8(1): 82–95. [PubMed: 23259582]

4. Hsiang YH, Liu LF. Identification of mammalian DNA topoisomerase I as an intracellular target of the anticancer drug camptothecin. Cancer Res. 1988; 48(7):1722–6. [PubMed: 2832051]
5. Pommier Y. Topoisomerase I inhibitors: camptothecins and beyond. Nature reviews Cancer. 2006; 6(10):789–802.
6. Seiler JA, Conti C, Syed A, Aladjem MI, Pommier Y. The intra-S-phase checkpoint affects both DNA replication initiation and elongation: single-cell and-DNA fiber analyses. Molecular and cellular biology. 2007; 27(16):5806–18. [PubMed: 17515603]
7. Antony S, Agama KK, Miao ZH, Takagi K, Wright MH, Robles AI, et al. Novel indenoisoquinolines NSC 725776 and NSC 724998 produce persistent topoisomerase I cleavage complexes and overcome multidrug resistance. Cancer Res. 2007; 67(21):10397–405. [PubMed: 17974983]
8. Martin SE, Wu ZH, Gehlhaus K, Jones TL, Zhang YW, Guha R, et al. RNAi screening identifies TAK1 as a potential target for the enhanced efficacy of topoisomerase inhibitors. Current cancer drug targets. 2011; 11(8):976–86. [PubMed: 21834757]
9. Nam EA, Cortez D. ATR signalling: more than meeting at the fork. The Biochemical journal. 2011; 436(3):527–36. [PubMed: 21615334]
10. Zeman MK, Cimprich KA. Causes and consequences of replication stress. Nat Cell Biol. 2014; 16(1):2–9. [PubMed: 24366029]
11. Jackson SP, Bartek J. The DNA-damage response in human biology and disease. Nature. 2009; 461(7267):1071–8. [PubMed: 19847258]
12. Smith J, Tho LM, Xu N, Gillespie DA. The ATM-Chk2 and ATR-Chk1 pathways in DNA damage signaling and cancer. Adv Cancer Res. 2010; 108:73–112. [PubMed: 21034966]
13. Charrier JD, Durrant SJ, Golec JM, Kay DP, Knegtel RM, MacCormick S, et al. Discovery of potent and selective inhibitors of ataxia telangiectasia mutated and Rad3 related (ATR) protein kinase as potential anticancer agents. Journal of medicinal chemistry. 2011; 54(7):2320–30. [PubMed: 21413798]
14. Toledo LI, Murga M, Zur R, Soria R, Rodriguez A, Martinez S, et al. A cell-based screen identifies ATR inhibitors with synthetic lethal properties for cancer-associated mutations. Nat Struct Mol Biol. 2011; 18(6):721–7. [PubMed: 21552262]
15. Reaper PM, Griffiths MR, Long JM, Charrier JD, Maccormick S, Charlton PA, et al. Selective killing of ATM- or p53-deficient cancer cells through inhibition of ATR. Nature chemical biology. 2011; 7(7):428–30.
16. Hall A, Newsome D, Wang Y, Boucher D, Eustace D, Gu Y, et al. Potentiation of tumor responses to DNA damaging therapy by the selective ATR inhibitor VX-970. Oncotargets. 2014; 5(14): 5674–85.
17. Peasland A, Wang LZ, Rowling E, Kyle S, Chen T, Hopkins A, et al. Identification and evaluation of a potent novel ATR inhibitor, NU6027, in breast and ovarian cancer cell lines. Br J Cancer. 2011; 105(3):372–81. [PubMed: 21730979]
18. Murga M, Campaner S, Lopez-Contreras AJ, Toledo LI, Soria R, Montana MF, et al. Exploiting oncogene-induced replicative stress for the selective killing of Myc-driven tumors. Nat Struct Mol Biol. 2011; 18(12):1331–5. [PubMed: 22120667]
19. Gilad O, Nabet BY, Ragland RL, Schoppy DW, Smith KD, Durham AC, et al. Combining ATR suppression with oncogenic Ras synergistically increases genomic instability, causing synthetic lethality or tumorigenesis in a dosage-dependent manner. Cancer Res. 2010; 70(23):9693–702. [PubMed: 21098704]
20. Huntoon CJ, Flatten KS, Wahner Hendrickson AE, Huehls AM, Sutor SL, Kaufmann SH, et al. ATR inhibition broadly sensitizes ovarian cancer cells to chemotherapy independent of BRCA status. Cancer Res. 2013; 73(12):3683–91. [PubMed: 23548269]
21. Prevo R, Fokas E, Reaper PM, Charlton PA, Pollard JR, McKenna WG, et al. The novel ATR inhibitor VE-821 increases sensitivity of pancreatic cancer cells to radiation and chemotherapy. Cancer biology & therapy. 2012; 13(11):1072–81. [PubMed: 22825331]
22. Fokas E, Prevo R, Pollard JR, Reaper PM, Charlton PA, Cornelissen B, et al. Targeting ATR in vivo using the novel inhibitor VE-822 results in selective sensitization of pancreatic tumors to radiation. Cell death & disease. 2012; 3:e441. [PubMed: 23222511]

23. Konig R, Chiang CY, Tu BP, Yan SF, DeJesus PD, Romero A, et al. A probability-based approach for the analysis of large-scale RNAi screens. Nature methods. 2007; 4(10):847–9. [PubMed: 17828270]
24. Jensen LJ, Kuhn M, Stark M, Chaffron S, Creevey C, Muller J, et al. STRING 8--a global view on proteins and their functional interactions in 630 organisms. Nucleic acids research. 2009; 37(Database issue):D412–6. [PubMed: 18940858]
25. Aris SM, Pommier Y. Potentiation of the novel topoisomerase I inhibitor indenoisoquinoline LMP-400 by the cell checkpoint and Chk1-Chk2 inhibitor AZD7762. Cancer Res. 2012; 72(4): 979–89. [PubMed: 22189968]
26. Shao RG, Cao CX, Shimizu T, O'Connor PM, Kohn KW, Pommier Y. Abrogation of an S-phase checkpoint and potentiation of camptothecin cytotoxicity by 7-hydroxystaurosporine (UCN-01) in human cancer cell lines, possibly influenced by p53 function. Cancer Res. 1997; 57(18):4029–35. [PubMed: 9307289]
27. Shao R-G, Cao C-X, Zhang H, Kohn KW, Wold MS, Pommier Y. Replication-mediated DNA damage by camptothecin induces phosphorylation of RPA by DNA-dependent protein kinase and dissociates RPA:DNA-PK complexes. EMBO J. 1999; 18:1397–406. [PubMed: 10064605]
28. Chou TC. Drug combination studies and their synergy quantification using the Chou-Talalay method. Cancer Res. 2010; 70(2):440–6. [PubMed: 20068163]
29. Conti C, Seiler JA, Pommier Y. The mammalian DNA replication elongation checkpoint: implication of Chk1 and relationship with origin firing as determined by single DNA molecule and single cell analyses. Cell cycle. 2007; 6(22):2760–7. [PubMed: 17986860]
30. Nam EA, Zhao R, Glick GG, Bansbach CE, Friedman DB, Cortez D. Thr-1989 phosphorylation is a marker of active ataxia telangiectasia-mutated and Rad3-related (ATR) kinase. J Biol Chem. 2011; 286(33):28707–14. [PubMed: 21705319]
31. Liu S, Shiotani B, Lahiri M, Marechal A, Tse A, Leung CC, et al. ATR autophosphorylation as a molecular switch for checkpoint activation. Molecular cell. 2011; 43(2):192–202. [PubMed: 21777809]
32. Bonner WM, Redon CE, Dickey JS, Nakamura AJ, Sedelnikova OA, Solier S, et al. gamma H2AX and cancer. Nat Rev Cancer. 2008; 8(12):957–67. [PubMed: 19005492]
33. Kinders R, Hollingshead MG, Lawrence S, Ji J, Tabb B, Bonner WM, et al. Development of a Validated Immunofluorescence Assay for γ H2AX as a Pharmacodynamic Marker of Topoisomerase I Inhibitor Activity. Clin Cancer Res. 2010
34. Solier S, Sordet O, Kohn KW, Pommier Y. Death receptor-induced activation of the Chk2- and histone H2AX-associated DNA damage response pathways. Mol Cell Biol. 2009; 29(1):68–82. [PubMed: 18955500]
35. Minn AJ, Rudin CM, Boise LH, Thompson CB. Expression of bcl-xL can confer a multidrug resistance phenotype. Blood. 1995; 86(5):1903–10. [PubMed: 7655019]
36. Frenzel A, Grespi F, Chmelewskij W, Villunger A. Bcl2 family proteins in carcinogenesis and the treatment of cancer. Apoptosis : an international journal on programmed cell death. 2009; 14(4): 584–96. [PubMed: 19156528]
37. Paik PK, Rudin CM, Brown A, Rizvi NA, Takebe N, Travis W, et al. A phase I study of obatoclax mesylate, a Bcl-2 antagonist, plus topotecan in solid tumor malignancies. Cancer chemotherapy and pharmacology. 2010; 66(6):1079–85. [PubMed: 20165849]
38. Okumura K, Huang S, Sinicrope FA. Induction of Noxa sensitizes human colorectal cancer cells expressing Mcl-1 to the small-molecule Bcl-2/Bcl-xL inhibitor, ABT-737. Clinical cancer research : an official journal of the American Association for Cancer Research. 2008; 14(24): 8132–42. [PubMed: 19088028]
39. Adhikari A, Xu M, Chen ZJ. Ubiquitin-mediated activation of TAK1 and IKK. Oncogene. 2007; 26(22):3214–26. [PubMed: 17496917]
40. Tokunaga F, Sakata S, Saeki Y, Satomi Y, Kirisako T, Kamei K, et al. Involvement of linear polyubiquitylation of NEMO in NF-kappaB activation. Nat Cell Biol. 2009; 11(2):123–32. [PubMed: 19136968]
41. Azzalin CM, Lingner J. The double life of UPF1 in RNA and DNA stability pathways. Cell cycle. 2006; 5(14):1496–8. [PubMed: 16861888]

42. Yasutis KM, Kozminski KG. Cell cycle checkpoint regulators reach a zillion. Cell cycle. 2013; 12(10):1501–9. [PubMed: 23598718]
43. Nghiem P, Park PK, Kim Ys YS, Desai BN, Schreiber SL. ATR is not required for p53 activation but synergizes with p53 in the replication checkpoint. J Biol Chem. 2002; 277(6):4428–34. [PubMed: 11711532]
44. Tse AN, Rendahl KG, Sheikh T, Cheema H, Aardalen K, Embry M, et al. CHIR-124, a novel potent inhibitor of Chk1, potentiates the cytotoxicity of topoisomerase I poisons in vitro and in vivo. Clin Cancer Res. 2007; 13(2 Pt 1):591–602. [PubMed: 17255282]
45. Zabludoff SD, Deng C, Grondine MR, Sheehy AM, Ashwell S, Caleb BL, et al. AZD7762, a novel checkpoint kinase inhibitor, drives checkpoint abrogation and potentiates DNA-targeted therapies. Mol Cancer Ther. 2008; 7(9):2955–66. [PubMed: 18790776]
46. Sordet O, Redon CE, Guirouilh-Barbat J, Smith S, Solier S, Douarre C, et al. Ataxia telangiectasia mutated activation by transcription- and topoisomerase I-induced DNA double-strand breaks. EMBO Rep. 2009; 10(8):887–93. [PubMed: 19557000]
47. Berniak K, Rybak P, Bernas T, Zarebski M, Biela E, Zhao H, et al. Relationship between DNA damage response, initiated by camptothecin or oxidative stress, and DNA replication, analyzed by quantitative 3D image analysis. Cytometry Part A : the journal of the International Society for Analytical Cytology. 2013; 83A:913–24.
48. Pires IM, Olcina MM, Anbalagan S, Pollard JR, Reaper PM, Charlton PA, et al. Targeting radiation-resistant hypoxic tumour cells through ATR inhibition. Br J Cancer. 2012; 107(2):291–9. [PubMed: 22713662]
49. Chanoux RA, Yin B, Urtishak KA, Asare A, Bassing CH, Brown EJ. ATR and H2AX cooperate in maintaining genome stability under replication stress. J Biol Chem. 2009; 284(9):5994–6003. [PubMed: 19049966]
50. Redon CE, Nakamura AJ, Gouliaeva K, Rahman A, Blakely WF, Bonner WM. The use of gamma-H2AX as a biodosimeter for total-body radiation exposure in non-human primates. PLoS One. 2010; 5(11):e15544. [PubMed: 21124906]

A

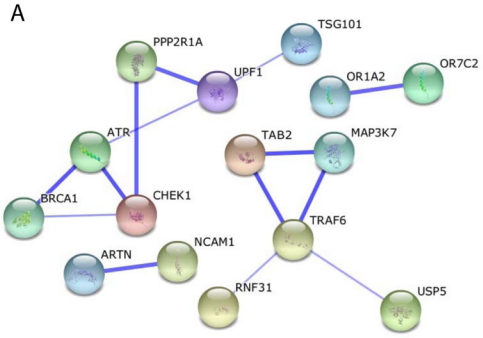

B

Gene	No. Active siRNAs	Median Fold Sens. of Active siRNAs
ATR	7 of 9	19
MAP3K7IP2	5 of 9	32
PPP2R1A	6 of 9	26
RNF31	6 of 9	14
TRAF6	5 of 7	22
UPF1	4 of 7	14
USP5	4 of 7	16

C

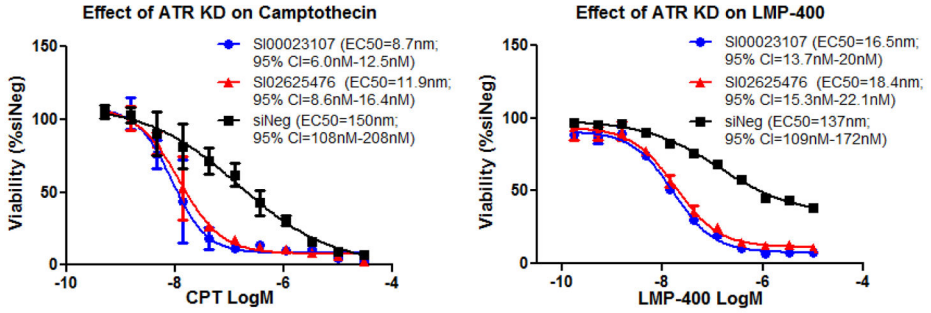

Figure 1. Druggable genome siRNA screen yields robust candidates whose knock down sensitizes MDA-MB-231 cells to CPT

(A) Top candidates are enriched in known protein-protein interactions as determined by STRING. A similar degree of high connectivity was observed by IPA (Supplemental Figure S1). **(B)** Testing ≥ 7 siRNAs for select candidates identified several genes with the majority of siRNAs leading to a ≥ 4-fold shift in CPT EC50 value. **(C)** The knockdown of ATR also sensitized MDA-MB-231 cells to LMP-400. Analysis was conducted with two active siRNAs (Qiagen) tested in panel B. ATR siRNAs n=3. Negative control siRNA (siNeg) n=16. Both siRNAs reduced *ATR* transcript levels by more than 80% as determined by real-time PCR. Catalog numbers are listed in the chart legends along with calculated EC50s and confidence intervals (CI).

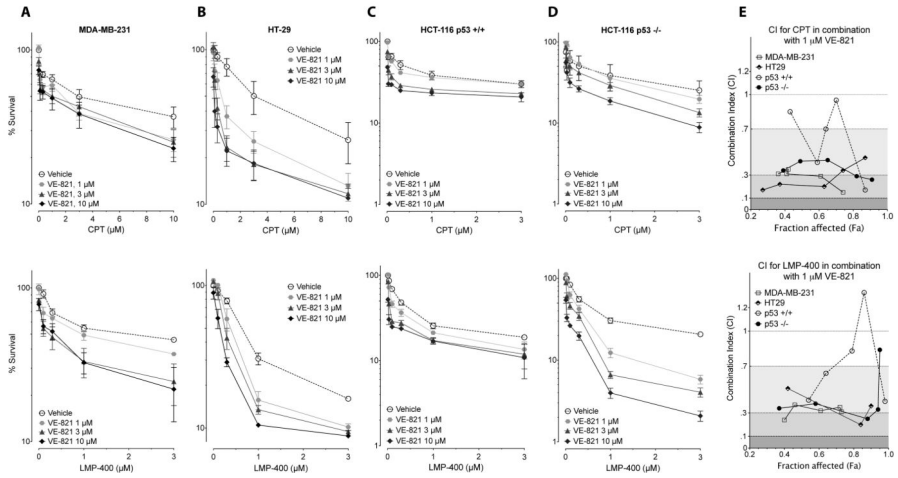

Figure 2. The ATR inhibitor VE-821 sensitizes to Top1 inhibitors under conditions where it is not cytotoxic by itself

(A–D) Viability of the indicated cell lines treated with CPT (upper panels A–D) or LMP-400 (lower panels A–D):**A**: MDA-MB-231; **B**: HT-29; **C**: HCT-116 control cells (p53 +/+); **D**: HCT-116 p53−/− cells. Cells were treated for 1 h with the combination of Top1 inhibitor without or with the indicated concentrations of VE-821. Top1 inhibitors were washed away and cells were grown in the presence or not of VE-821 for 72 h. (**E**) Graph of CI (Combination Index) values versus Fa (Fraction affected) for data points of CPT (top panel) or LMP-400 (lower panel) in combination with 1 μM VE-821. Shading reflects the level of synergism. CI values between 0.7 and 0.3, CI between 0.3 and 0.1 and CI less than 0.1 indicate synergy, strong synergy and very strong synergy, respectively.

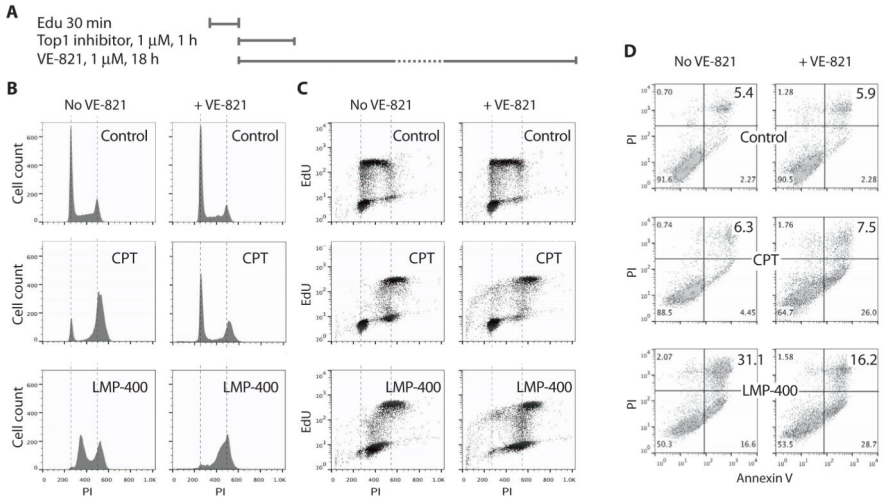

Figure 3. S-phase arrest induced by CPT or LMP-400 is abrogated by VE-821

(**A**) Experimental protocol. (**B**) Cell cycle effects were determined by propidium iodide (PI) staining. Vertical dashed lines correspond to 2N and 4N DNA contents. (**C**) S-phase progression was monitored by following the cells that were replicating (EdU-labeled) at the time of Top1 inhibitor treatment. (**D**) Effect of VE-821 on apoptotic cells48 h after Top1 inhibitors removal. Annexin V/PI double staining was used to monitor apoptosis.

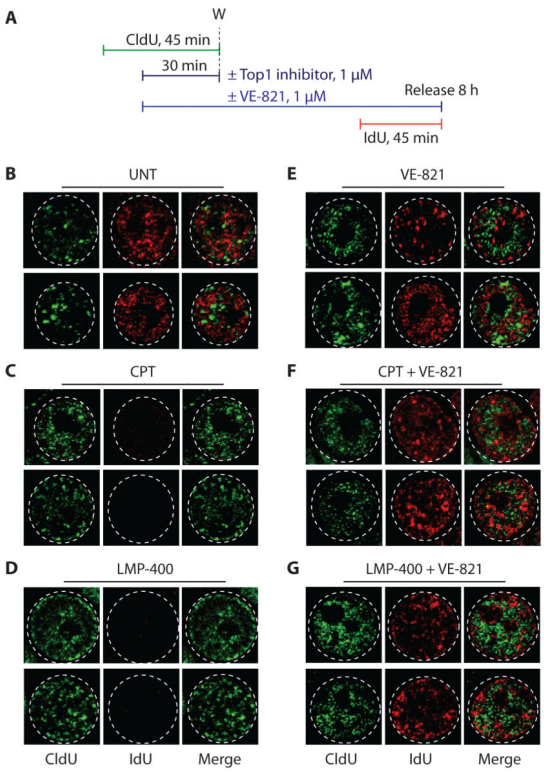

Figure 4. VE-821 reactivates replication foci activity and firing in cells treated with the Top1 inhibitors, CPT andLMP-400

(**A**) Experimental protocol. (**B** to **G**) Confocal images of representative cell nuclei immediately after the IdU pulse (see panel A). (**B**) Untreated cells, (**C**) CPT alone, (**D**) LMP-400 alone, (**E**) VE-821 alone, (**F**) co-treatment with VE-821 and CPT, and (**G**) co-treatment with VE-821 and LMP-400.

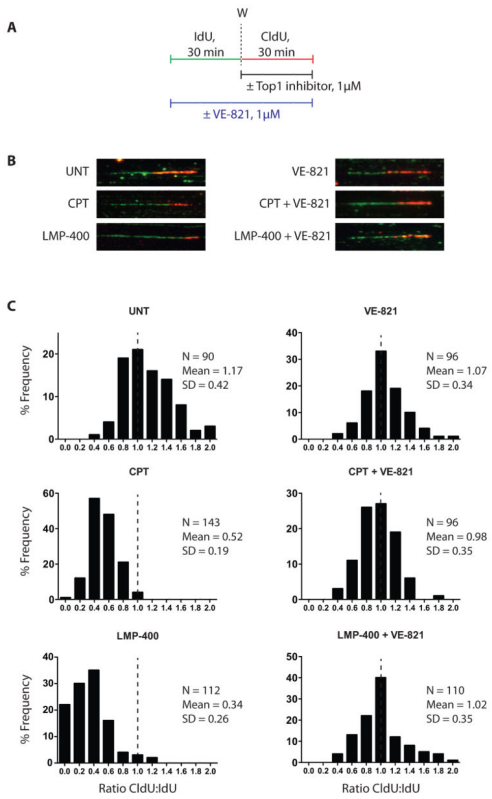

Figure 5. VE-821 restores replication fork elongation in cells treated with CPT orLMP-400

(**A**) Experimental protocol. IdU and CldU were added sequentially to the cell cultures for 45 min each and visualized in green and red, respectively. Top1 inhibitors were added during the CldU pulse while the ATR inhibitor was present during both pulses. (**B**) Representation images of molecular combing. (**C**) Histograms showing the distribution of elongation ratios calculated for each condition.

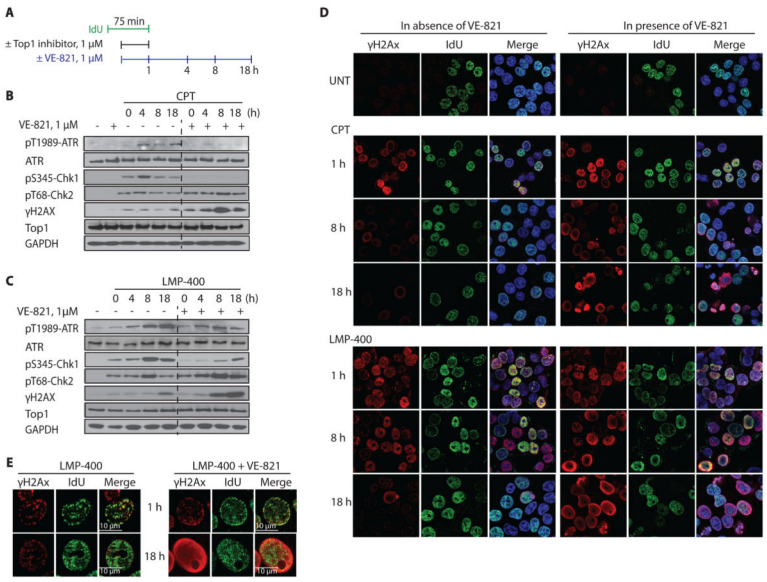

Figure 6. VE-821 inhibits the ATR-Chk1 response and induces intense and diffuse γH2AX staining

(**A**) Experimental protocol. (**B**) Kinetics of ATR activation (phosphorylation on threonine 1989), Chk1 activation (phosphorylation on serine 345), Chk2 activation (phosphorylation on threonine 68) and γH2AX analyzed by immunoblotting. GAPDH was used as loading control. (**C**) Same as panel B forLMP-400 instead of CPT. (**D**) Representative confocal images after treatment with Top1 inhibitors (1 h) or 8 and 18 h after removal of the indicated Top1 inhibitors. IdU was incorporated 15 m in before and during Top1 inhibitors treatments. γH2AX pattern was examined in replicating and non-replicating cells. (**E**) Confocal images of representative nuclei for LMP-400 alone (left panels) or LMP-400 in combination with VE-821. Upper panel: at the end of LMP-400 treatment; lower panels: 18 h post Top1 inhibitor removal.

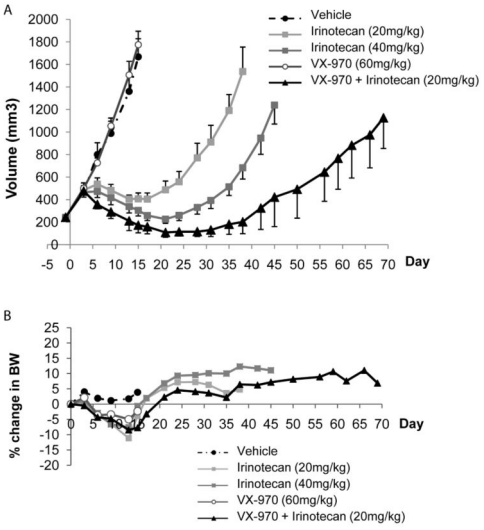

C

Study Group	Impact on tumor growth		Max body weight loss (%)
	TGI[a] on d15 (%)	Regression[b] on d21 (%)	
Vehicle	-	-	-
Irinotecan (20 mg/kg)	88	-	-11
Irinotecan (40 mg/kg)	96	-6	-7.6
VX-970 (60 mg/kg)	0	-	-5
Irinotecan (20 mg/kg) + VX-970 (60 mg/kg)	-29	-55	-8.5

Figure 7. The clinical ATR inhibitor VX-970 potentiates the efficacy of irinotecan in the colorectal cancer COLO205 mouse xenograft model

Mice bearing COLO205 tumors (volume ~250 mm3) were treated with vehicle, irinotecan (20 mg/kg or 40 mg/kg administered by intraperitoneal bolus injection on day 0 of each 4 day cycle), VX-970 (60 mg/kg administered by oral gavage on days 0, 1 and 2 of each 4 day cycle), or the combination of both drugs (using the schedule for administration of each compound alone). Treatment was continued for 4 cycles. Each group consisted of 8 mice. Animals receiving irinotecan or the combination of irinotecan and VX-970 were allowed to recover after treatment to assess tumor regrowth. (**A**) Tumor size, assessed twice a week. (**B**). Body weight throughout the study. (**C**). Table summarizing effect of irinotecan and VX-970 on tumor growth and body weight. a) TGI is tumor growth inhibition calculated as 100-%T/C where %T/C is the ratio of tumor growth on drug treatment (T) to vehicle treated controls (C). b) Regression is calculated as the ratio of final tumor volume (T) to starting tumor volume (Ti) expressed as a percentage.